International Journal of Applied and Natural Sciences (IJANS)
ISSN(P): 2319-4014; ISSN(E): 2319-4022
Vol. 3, Issue 2, Mar 2014, 115-134

International Academy of Science, Engineering and Technology
Connecting Researchers; Nurturing Innovations

THE SUBSTITUTED *N*-NITROSO PIPERIDIN-4-ONES: A NEW CLASS OF INHIBITORS OF MILD STEEL IN ACID MEDIUM

A. ILAMPARITHI[1], A. SELVARAJ[2] & S. PONNUSWAMY[3]

[1,3]PG and Research, Department of Chemistry, Government Arts College (Autonomous), Coimbatore, Tamil Nadu, India

[1]Department of Chemistry, Gobi Arts and Science College (Autonomous), Gobichettipalayam, Tamil Nadu, India

[2]PG and Research, Department of Chemistry, CBM College, Coimbatore, Tamil Nadu, India

ABSTRACT

The *N*-nitroso piperidin-4-ones synthesized in the laboratory were used to study the effect of corrosion of mild steel in 1N H_2SO_4 and 1N HCl. Weight loss and electrochemical techniques were used to monitor the corrosion behaviour on mild steel. The results so obtained reveal that all the *N*–nitroso derivatives are excellent corrosion inhibitors for low carbon steel in 1N H_2SO_4 and 1N HCl. Potentiodynamic polarization studies have shown that all these compounds suppress both anodic and cathodic process and behave as mixed type inhibitors. The ac impedance studies indicate that the adsorption process is involved in corrosion inhibition. The adsorption of these compounds on mild steel surface is found to obey Langmuir adsorption isotherm and Tempkin adsorption isotherm. The adsorbed compounds were characterized by FT-IR spectra. The surface morphology was also studied by SEM as well as EDS analysis. The results were corroborated by measuring thermodynamic parameters.

KEYWORDS: FT-IR, Mild Steel (MS), *N*-nitroso Piperidones, Nyquist Plots, Polarization Curve, SEM/EDS, Tafel Plots

INTRODUCTION

Acid solutions are widely used for the removal of undesirable scale and rust on metal surfaces in several industrial process. Inhibitors are employed in this process to control the corrosion rate of the metals. Most of the well known acid inhibitors are organic compounds containing nitrogen, oxygen and sulphur atoms. The available literature on corrosion shows that these compounds can adsorb on the mild steel surface and block the active sites and thereby decreasing the corrosion process. Many piperidin-4-one compounds have been proved to be effective inhibitors for the corrosion of carbon steel in acid media [1-5]. In continuation of our work on the discovery of a new class of piperidin-4-one based inhibitors[5], the present work involves the study of the inhibition efficiency of certain *N*-nitroso piperidin-4-ones *viz*, *t*-3-methyl-*N*-nitroso-*r*-2,*c*-6-diphenylpiperidone (N3MPO), *t*-3-ethyl-*N*-nitroso-*r*-2,*c*-6-diphenylpiperidone (N3EPO), *t*-3-isopropyl-*N*-nitroso -*r*-2,*c*-6-diphenylpiperidone (N3IPPO) and *t*-3,*c*-5-dimethyl-*N*-nitroso-*r*-2,*c*-6-diphenylpiperidone (NDMPO) for carbon steel corrosion in acid medium.

In the present work, we have investigated the effect of addition of N3MPO, N3EPO, N3IPPO and NDMPO on the corrosion inhibition of mild steel in 1N H_2SO_4 and 1N HCl by weight loss, electrochemical impedance spectroscopy and potentiodynamic polarization measurements. Adsorbed material on the metal surface was analyzed by FT-IR, SEM and EDS analysis. Adsorption mode and corrosion inhibition mechanism on the steel surface were discussed.

MATERIALS AND METHODS

Synthesis of the Inhibitors

N-Nitroso piperidin-4-ones were synthesized by following the reported experimental procedure[6-17]. The chemical structures of the inhibitors are given in Figure 1.

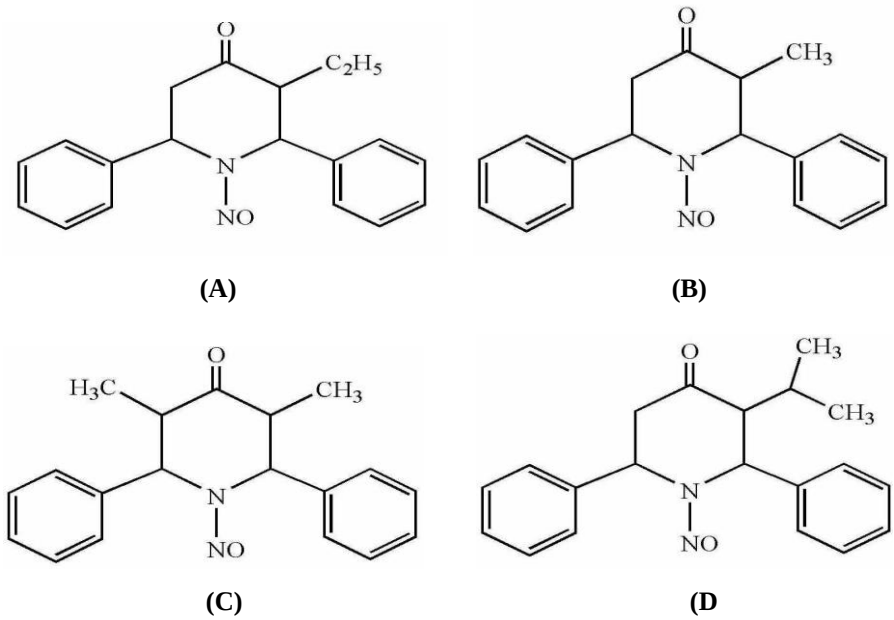

Figure 1: Structure of the Inhibitors (A) N3MPO, (B) N3EPO, (C) N3IPPO, (D) NDMPO

Gravimetric Measurements

For the weight loss measurements, mild steel rods of chemical composition 0.224% C, 0.025% Si, 0.320% Mn, 0.023% P, 0.052% S, 0.108% Ni, 0.069% Cr, 0.012% Mo, 0.047% Al, 0.011% Cu, the remainder being Fe and of size 2.5cm x 1cm x 0.1cm were used. The samples were polished mechanically using 100, 200, 400, 600, 800 grade wet SIC emery paper, rinsed with double distilled water, degreased in tricholoroethene. The cleaned samples were weighed before and after immersion in 100 ml of 1N H_2SO_4 and 1N HCl for 3 hours in the absence and the presence of various concentrations of *N*-nitroso piperidone derivatives. The efficiency was also studied by raising the temperature up to 323K and also recorded by increasing the immersion time up to 24 h. The corrosion rate (mm/Y), surface coverage [θ] and inhibition efficiency were calculated from the difference in weight loss values. Since the solubility of inhibitor is less and in order to avoid precipitation, 40 ml ethyl alcohol, was used to make up the solution, for all gravimetric and electrochemical studies.

Electrochemical Analysis

The potentiodynamic polarization studies and electrochemical impedance measurements were performed using Potentiostat/ Galvanostat/ FRA2 (μ Autolab type 3). Mild steel working electrode embedded in Teflon with an exposed area of 1 cm^2 was used as a working electrode. Auxiliary electrode was a platinum electrode and saturated calomel electrode was used as a reference electrode. The electrodes used for electrochemical analysis were polished to a mirror finish using 200, 400, 600, and 800 grade emery papers and degreased with acetone. After measuring the open circuit potential, potentiodynamic polarization curves were obtained with a scan rate of 1mV s^{-1} in the potential range from -200 mV to +200 mV with respect to the corrosion potential. Corrosion current density values were obtained by

Tafel extrapolation method. Electrochemical impedance measurements were performed at 30 ± 1° C and at open circuit potential, before taking potentiodynamic polarization measurements. The superimposed ac signal has the frequency range from 100 KHz to 1 Hz and is produced using sine wave generated by an Ivium frequency response analyzer with a signal amplitude perturbation of 10 mV.

RESULTS AND DISCUSSIONS

Weight Loss Measurements

From the experimental weight loss data the percentage inhibition efficiency (IE%) was calculated using the formula:

$$IE(\%) = \frac{W_o - W}{W_o} \times 100 \quad (1)$$

Where W_o and W are the weight loss observed in the absence and in the presence of inhibitor, respectively. The values of percentage inhibition, corrosion rate and surface coverage for all investigated concentrations of N3MPO, N3EPO, N3IPPO and NDMPO are summarized in Table 1. It is found that both the weight loss and corrosion rate decreases with the increase in concentration of the inhibitor. The *N*-nitroso piperidin-4-ones inhibit better in HCl than in H_2SO_4. The inhibiting efficiency trend is as follows:

N3IPPO > N3EPO > N3MPO > NDMPO. The same trend was proposed by Sankarapapavinasam *et al.*[2] for piperidones with no substitution on the nitrogen atom. Furthermore, we have observed the similar trend in the case of *N*-formyl piperidin-4-ones.[5] The possible explanation is that the alkyl groups are known to produce +I effect and the electron releasing tendency increases with the increase in carbon number of the alkyl group. The isopropyl group raises the electron density both on the carbonyl oxygen and nitrogen atom of the piperidone ring, which in turn facilitates better adsorption on the MS surface thereby increasing its protection efficiency.

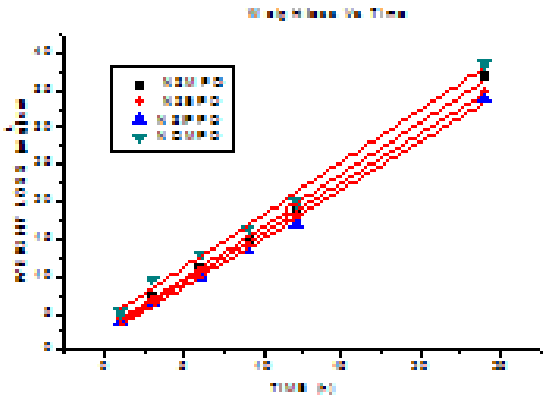

Figure 2: Variation of Weight Loss of MS in 1N H_2SO_4 with Immersion Time

The results presented in Table 2 and Table 4, clearly reveal that the weight loss and corrosion rate increases linearly with the increase in immersion time and temperature for both the presence and the absence of inhibitor and also shown in Figure 2. However, the inhibiting efficiency (IE%) increased upto 12 h and almost remains the same thereafter. This can be attributed to increase in exposure time; all the anodic and cathodic sites are completely adsorbed by the inhibitor molecule and the available active site fraction 1-Θ is equal to surface covered fraction Θ, therefore the rate of adsorption and desorption remains constant after 12 h. [18]

Effect of Addition of 1 mM Anions on the Corrosion Inhibition of MS in H_2SO_4

The effect of anions on the inhibition efficiency (IE) of organic compounds were studied by several authors [5, 19-21] and they observed that the synergistic effect increased in the order $Cl^-<Br^-<I^-$. Similar trend prevails in our study also; the results are shown in Table 3. The other anions like nitrate ion and thiocyanide ion have no appreciable synergistic effects. According to Damaskin and co-workers.[22] the steel surface is originally positively charged at the open circuit potential (-500 mV / SCE) in H_2SO_4 due to the weak adsorption of the highly solvated SO_4^{2-} ions. Under these conditions the cationic protonated inhibitor molecules are not adsorbed strongly. Only the neutral inhibitor molecules hold on to the anionic metal active centres. When the halide ions are added, they are strongly chemisorbed on the metal surface by entering into the metallic part of the double layer there by shifts the potential of zero charge ϕ_n towards more positive potentials. As a result the metal surface at the open circuit potential becomes negatively charged. Once the surface is negatively charged, the cationic inhibitor molecule is strongly adsorbed on the metal surfaces thus enhance its protective action.

The synergism parameter 'S' has been defined by Aramaki et al., [23] by the relation

$$S = \frac{1- I_{1+2}}{1- I'_{1+2}} \qquad (2)$$

Where I'_{1+2} = measured inhibition efficiency of anions plus cations.

$I_{1+2} = I_1 + I_2$

I_1 = Inhibition efficiency of the anions

I_2 = Inhibition efficiency of the cations (inhibitors)

The significance of synergism parameter 'S' is that "a value of S>1 denotes synergism while a value of S<1 denotes antagonism". The synergism parameters calculated for all the inhibitors are greater than 1 for halide ions and less than 1 for nitrate ions. Further the S value increases in the order $Cl^-<Br^-< I^-$ giving highest synergistic influence for I^- which is in accordance with the findings noted in the literature. [5,19-21]

Effect of Temperature

In order to study the effect of temperature on the inhibition characteristic of *N*-nitroso piperidone derivatives gravimetric experiments were conducted at 303, 308, 313, 318 and 323K in 1N H_2SO_4 in presence of 1mM inhibitors concentration and the data obtained are presented in Table 4. Analysis of this data reveals that inhibition efficiencies were found to increase as the temperature increased upto 323K.

The data obtained from weight loss measurements were plotted in accordance with the Arrhenius Equation:

$$\text{Log CR} = -\frac{E_a}{2.303\ RT} + A \qquad (3)$$

Where E_a is the activation energy, R is the universal gas constant, A is the Arrhenius frequency factor and CR is the corrosion rate. A plot of Log CR versus T^{-1} gives a straight line and is shown in Figure 3.

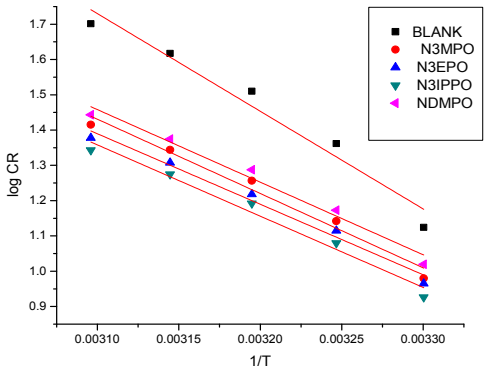

Figure 3: The Arrhenius Plots of MS Corrosion in 1N H_2SO_4 Solution Containing Inhibitors

The activation ($Ea_)$ energy is calculated from the slope of the line which is $\frac{E_a}{2.303\ R}$

An alternative formulation of Arrhenius equation is the transition state equation:

$$CR = \frac{RT}{Nh} \exp\left(\frac{\Delta S^{\#}}{R}\right) \exp\left(\frac{-\Delta H^{\#}}{RT}\right) \quad (4)$$

Where N is the Avogadro's number, h is the Planck's constant, $\Delta S^{\#}$ is the entropy of activation and $\Delta H^{\#}$ is the enthalpy of activation.

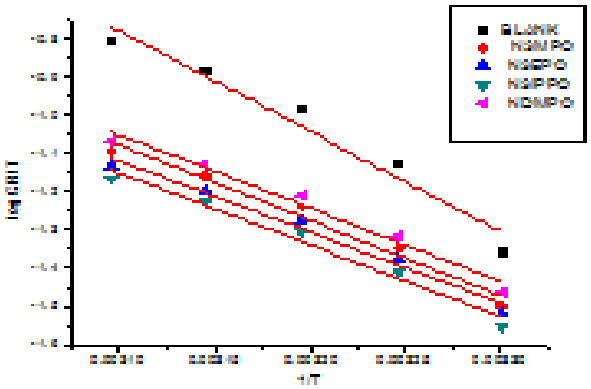

Figure 4: The Transition State of MS Corrosion in 1N H_2SO_4 Solution Containing Inhibitors

A plot of log (CR / *T*) versus 1 / *T* should give a straight line (Figure 4) with a slope of $(-\Delta H^{\#}/2.303R)$ and an intercept $(\log R / Nh + \Delta S^{\#}/2.303R)$ from which the values of $\Delta S^{\#}$ and $\Delta H^{\#}$ were calculated.

It is observed from Table 5 that the activation energy is lower in the presence of inhibitor than in its absence. The low activation energy values support the low value of I_{corr} obtained from polarization measurements and that indicates the higher protective efficiency of the inhibitor. For this type of inhibitor, inhibition is higher at ordinary temperature, but decreased at elevated temperatures. The sign of $\Delta H^{\#}$ predicts the exothermic nature of the corrosion process. The entropy of activation, $\Delta S^{\#}$, in the absence and presence of inhibitor is negative. This implies that the activated complex in the rate determining step represents association rather than dissociation. These results denote that the energy barrier for the corrosion reactions decreases as the concentration of inhibitor is increased.

From the expression $\Delta G^{o}_{ads} = -RT\ln(55.5x\ K)$,

(where the equilibrium constant

K is equal to $\left(\frac{\theta}{(1-\theta)\,C} \right)$ (5)

ΔG^{o}_{ads} can be calculated and it is presented in Table 6. The negative values of ΔG^{o}_{ads} and positive value of $\Delta H^{\#}$ indicate the strong interaction and spontaneous adsorption of the inhibitor molecules on the mild steel surface [24, 25]. These thermodynamic data imply the formation of the chemical bond between the inhibitor molecule and the metal surface through charge transfer or charge sharing [2, 3, 5, 26].

The Electrochemical Impedance Spectroscopy (EIS)

The corrosion behaviour of mild steel in 1N H_2SO_4 and 1N HCl in presence of various concentrations of N3MPO, N3EPO, N3IPPO and NDMPO was investigated by the EIS and Nyquist plots obtained are shown in Figures 5, 6, 7, 8 and 9. Since all the compounds show similar spectrum, representative plots for N3MPO, N3EPO, N3IPPO and NDMPO are shown. The charge transfer resistance, $R_{ct,}$ values are calculated from the difference in impedance at lower and higher frequencies, as suggested by Tsuru and Haruyama [27]. To obtain the double layer capacitance (C_{dl}), the frequency at which the imaginary component of the impedance ($-z''_{max}$) is maximum is found and C_{dl} values are obtained from the following equation.

$$-z''_{max} = 1 / 2\pi f (C_{dl})\, R_{ct} \quad (6)$$

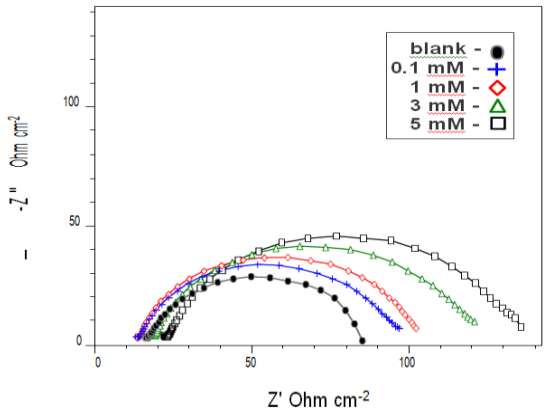

Figure 5: The Nyquist Plots for MS in 1N H_2SO_4 in the Presence and in the Absence of N3EPO

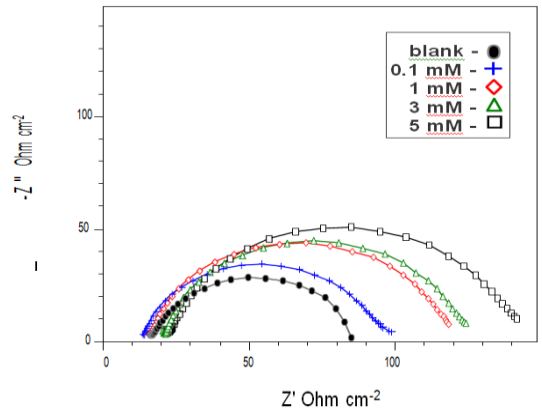

Figure 6: The Nyquist Plots for MS in 1N H_2SO_4 in the Presence and in the Absence of N3IPPO

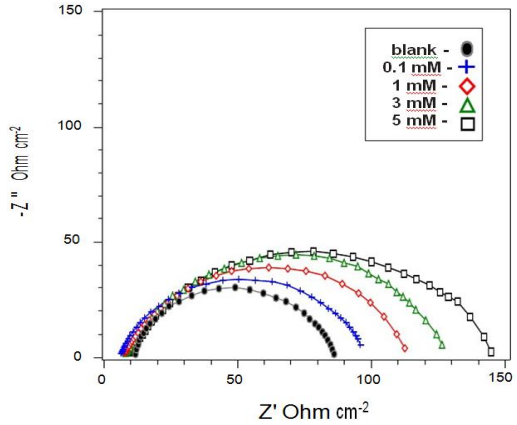

Figure 7: The Nyquist Plots for MS in 1N HCl in the Presence and in the Absence of N3IPPO

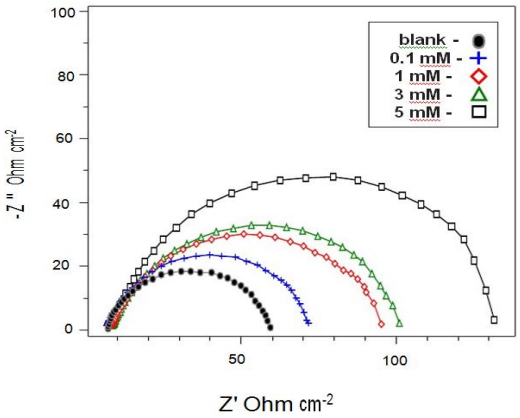

Figure 8: The Nyquist Plots for MS in 1N HCl in the Presence and in the Absence of N3MPO

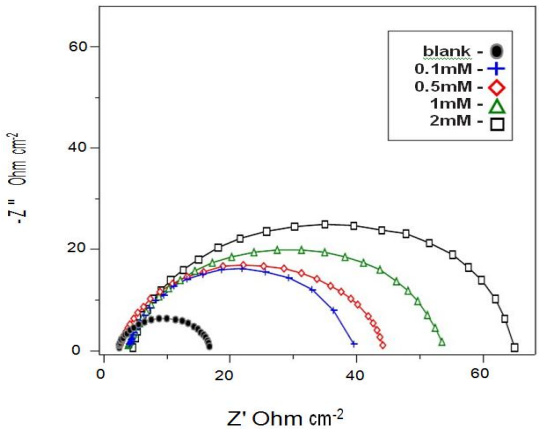

Figure 9: The Nyquist Plots for MS in 1N HCl in the Presence and in the Absence of NDMPO

The impedance parameters derived from these investigations are given in Table 7 & 8. It is found that as the concentration of the inhibitors N3MPO, N3EPO, N3IPPO and NDMPO increases, the R_{ct} values increases but the C_{dl} values tend to decreases. As can be seen from Table 7 and 8, R_{ct} values and inhibition efficiencies are increased with increasing the concentrations of *N*-nitroso piperidone derivatives. The organic molecules inhibit the corrosion process either by diffusion process or by activation process. The charge transfer controlled Nyquist plot gives a linear pattern for a diffusion controlled inhibition and a semi-circular loop for the activation controlled inhibition process. As all the Nyquist curves appear as semi-circular loops, it can be concluded that inhibition by *N*-nitroso piperidone derivatives on mild steel is activation controlled. The efficiency of all inhibitors increases with the increase in concentration.

Potentiodynamic Polarisation Measurements

Representative Tafel polarisation curves of mild steel in 1N HCl and in 1N H_2SO_4 solutions with different concentrations of N3MPO, N3EPO, N3IPPO and NDMPO are shown in Figures 10, 11, 12, 13 and 14. Electrochemical parameters obtained from the Tafel extrapolation method using polarisation curves are given in Tables 7 and 8.

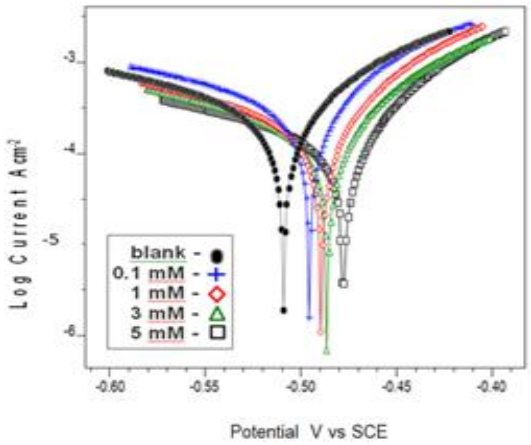

Figure 10: The Tafel Plots for MS in 1N H_2SO_4 in the Presence and in the Absence of N3EPO

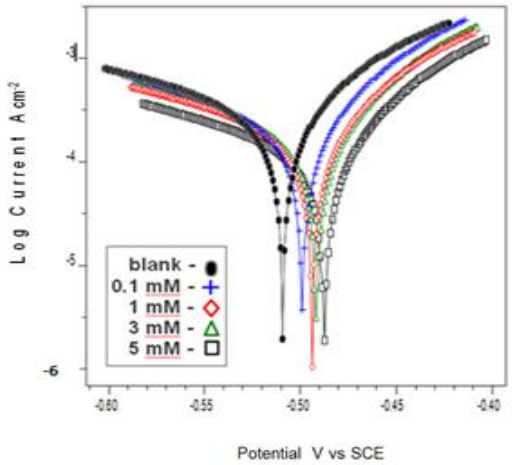

Figure 11: The Tafel Plots for MS in 1N H_2SO_4 in the Presence and in the Absence of N3IPPO

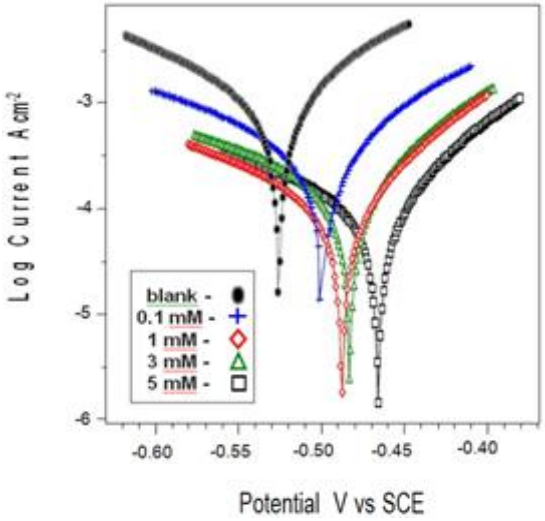

Figure 12: The Tafel Plots for MS in 1N HCl in the Presence and in the Absence of N3IPPO

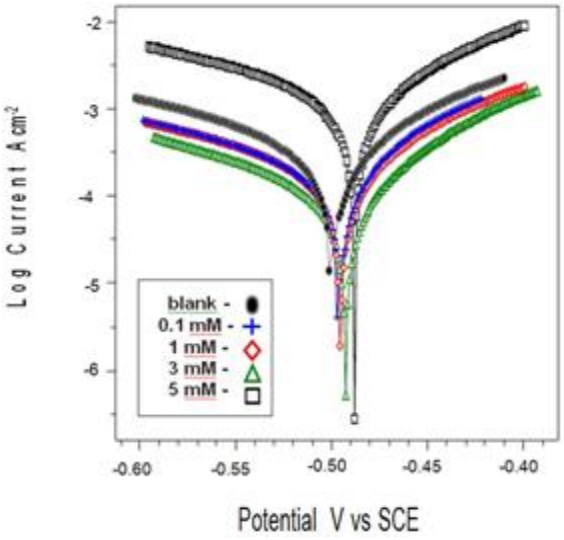

Figure 13: The Tafel Plots for MS in 1N HCl in the Presence and in the Absence of N3MPO

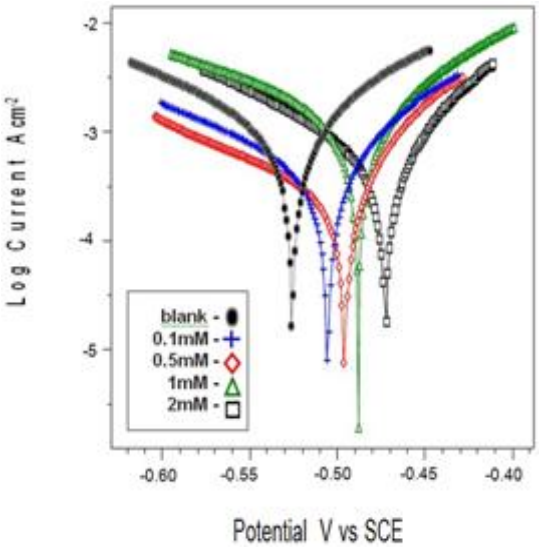

Figure 14: The Tafel Plots for MS in 1N HCl in the Presence and in the Absence of NDMPO

Corrosion currents obtained in 1N H_2SO_4 and in 1N HCl solutions with *N*-nitroso piperidones are lower than corrosion currents obtained in acid solution without the inhibitors. Increase in concentration of added *N*-nitroso piperidone derivatives causes shifting of corrosion potentials towards noble direction and variation in both the Tafel slopes. But cathodic and anodic Tafel slopes are equally enhanced; hence inhibition of corrosion on carbon steel in 1N H_2SO_4 and in 1N HCl solution by the *N*-nitroso piperidin-4-ones is under mixed control without affecting the mechanism of cathodic hydrogen evolution and anodic metal dissolution. An increase in inhibition efficiencies with the increase in concentrations of *N*-nitroso piperidin-4-ones shows that the inhibition actions are due to adsorption on steel surface.

ADSORPTION ISOTHERM AND INHIBITION MECHANISM

The corrosion inhibitive action of the inhibitor molecules in acid media on mild steel is due to its adsorption at the metal solution interface. The adsorption of the organic compounds can be described by two main types of interactions *viz.*, physical adsorption and chemical adsorption; these are influenced by the nature and charge of the metal, the chemical structure of the inhibitor and type of electrolyte.

Chemisorption involves charge sharing or charge transfer from the inhibitor molecule to the mild steel surface to form a coordinate covalent type bond. The electron transfer is reckoned for transition metals having vacant, low-energy electron orbital. Inhibition efficiency depends on several factors such as the number of adsorption sites and their charge density, molecular size of the inhibitor molecule, mode of interaction with the metal surface and formation of metallic complexes.

As the process of inhibition occurs through the phenomenon of adsorption, it is necessary to develop suitable mechanism for the adsorption of *N*-nitroso piperidin-4-ones on the carbon steel surface. Damaskin and co-workers [22] have suggested that adsorption of organic molecule on different type of metallic surfaces occurs through competitive adsorption between organic compound and water molecules. The higher free energy of adsorption for organic compounds than for water molecule facilitates such adsorption. Sankarapapavinasam *et al.*[2] have analysed the adsorption of piperidine and a few piperidones on the corrosion of copper and sulphuric acid. They averred that the interaction of piperidone with the metal surface could occur through >C=O or –NH group, the lower electronegativity of the nitrogen atom favours –NH as an anchoring site with chair conformation, but involvement of both -NH and >C=O groups was ruled out by them as it would need the piperidones to be in strained boat conformation. Muralidharan *et al.*[1] and Mallika *et al.*[28] have also concluded that piperidones adsorb through nitrogen lone pair in chair conformation.

However, Ravichandran *et al.*[29] have proposed that piperidones adsorbed through both -N and >C=O group with strained boat conformation with the aid of IR spectral studies. The carbonyl adsorption peak around 1700 cm^{-1} has disappeared completely while N-H stretching band around 3300 cm^{-1} and C-N stretching 1000-1350 cm^{-1} have been altered. A new O-H stretching band around 3000-3500 cm^{-1} has appeared. The above observation indicated that after the adsorption of inhibitor on mild steel surface the carbonyl group is reduced catalytically to C-OH group, with axial orientation of alcohol, in order to facilitate the continued adsorption in the boat form.

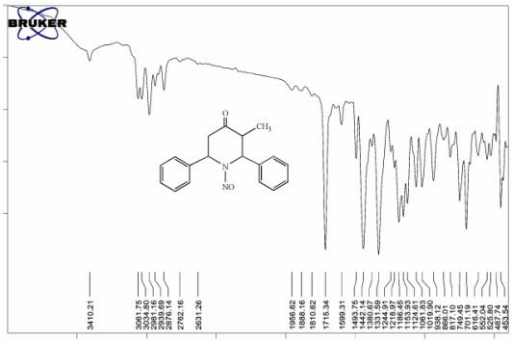

Figure 15(a): N3MPO

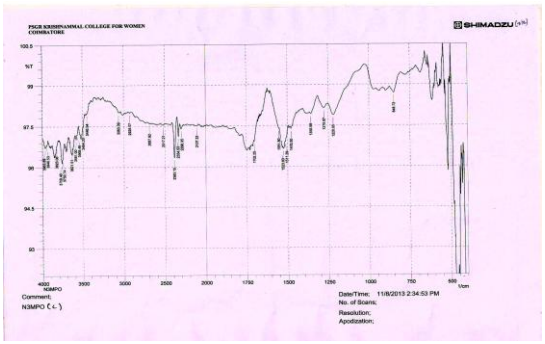

Figure 15(b): N3MPO (Compound)

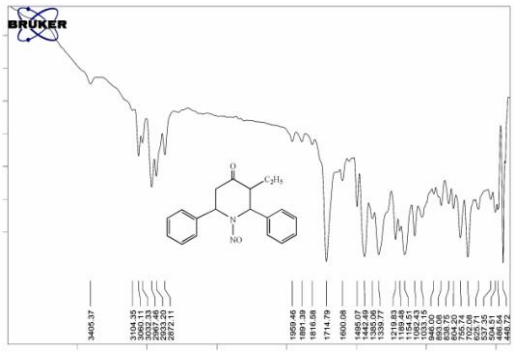

Figure 16(a): N3EPO

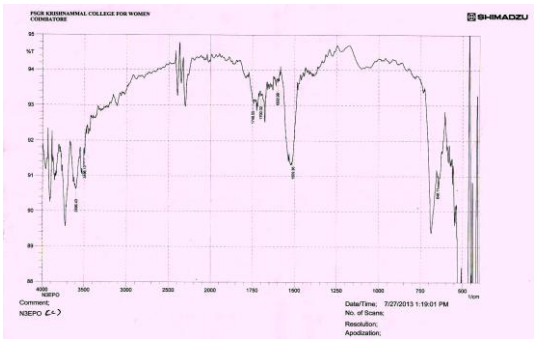

Figure 16(b): N3EPO (Compound)

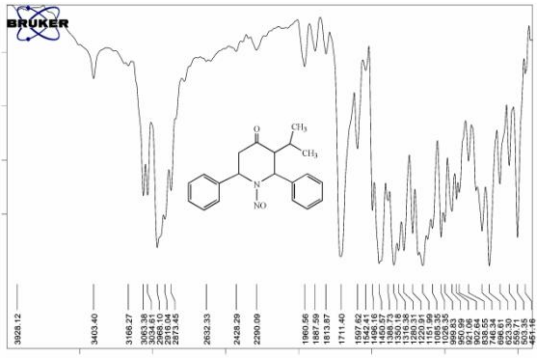

Figure 17(a): N3IPPO

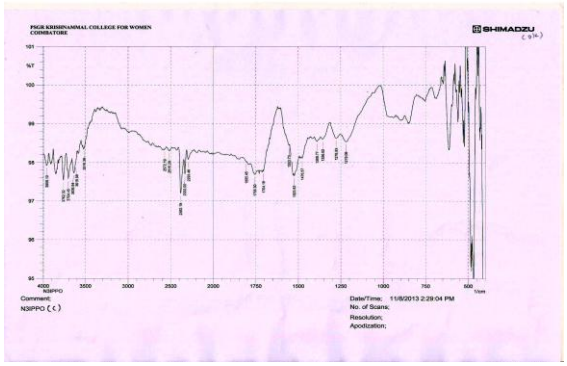

Figure 17(b): N3IPPO (Compound)

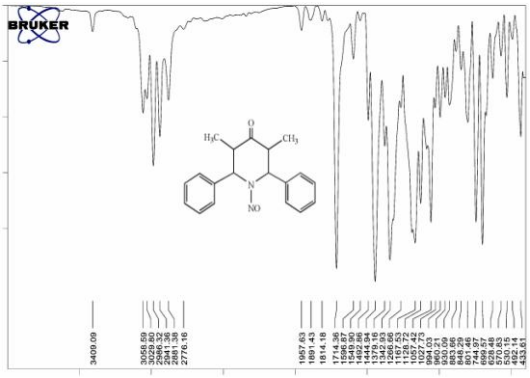

Figure 18(a): NDMPO

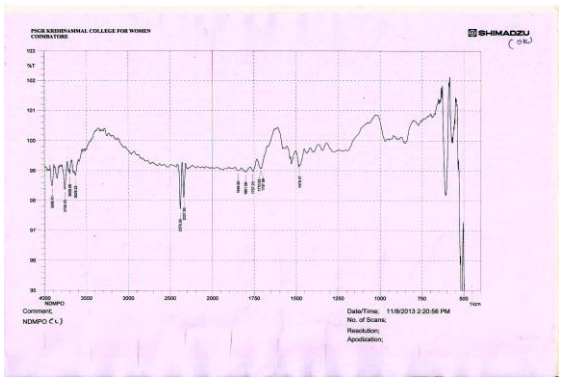

Figure 18(b): NDMPO (Compound)

FTIR Spectrum of the Material Scrapped from MS Surface (b) and FTIR Spectrum of the Parent Compounds Are (a)

The FT-IR spectra of the parent inhibitor molecules in this study *viz*., N3MPO, N3EPO, N3IPPO and NDMPO were recorded using Perkin-Elmer 1600 FT-IR spectrometer and are shown in the Figures 15a, 16a, 17a, and 18a. All the parent inhibitor molecules show a sharp ring carbonyl peak around 1710 - 1716 cm^{-1} and a peak corresponding to -N=O group at 1440 - 1451 cm^{-1}. The IR spectra of adsorbed compounds are shown in Figures 15b to 18b. The nitroso peak has completely disappeared in the adsorbed material and the carbonyl peak is shifted to 1510 - 1525 cm^{-1}, clearly indicates that the carbonyl oxygen as well as the nitroso oxygen is the anchoring sites. In the IR spectra of entire product molecules, a prominent new peak appears around 3600 - 3750 cm^{-1}. As discussed earlier, the carbonyl group gets reduced to OH group which accounts for this peak[5]. The peak around 3600 - 3750 cm^{-1} could be due to strained axial OH stretching which is linked to MS surface.

The *N*-nitroso piperidin-4-ones have been reported to adopt a twist-boat conformation in the solution as well as the solid states with the coplanar orientation of the -*N*-N=O function due to the effective delocalisation of lone pair of electrons on nitrogen into the -N=O π- cloud [6-11, 15, 16] (Figure 19). Furthermore, the change of hybridisation of the ring nitrogen from sp^3 to sp^2 is possible only in the coplanar orientation of the *N*-nitroso group and the bond angle around the nitrogen was found to be around 120º. In order to get adsorbed on the MS surface, the piperidone ring would have shifted to a flattened boat conformation as shown in Figure 20 and the -*N*-N=O moiety apparently retains the coplanar orientation. However, the degree of coplanarity of the *N*-N=O function with respect to the C2-N1-C6 plane of the molecule would be expected to be less when compared to the free *N*-nitroso piperidin-4-ones.

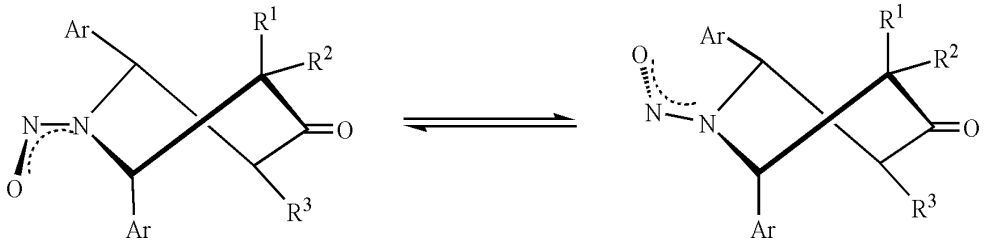

Figure 19: Twist-Boat Conformation of *N*-nitroso Piperidin-4-Ones

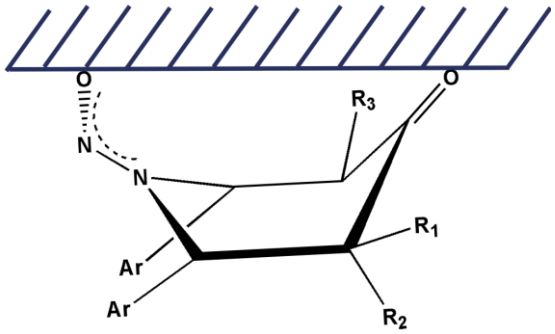

Figure 20: Mode of Adsorption of *N*-nitroso Piperidin-4-Ones on the MS Surface in the Flattened Boat Conformation

The lone pair of electrons on the nitrogen atom of the piperidin-4-ones have been reported to involve a strong delocalisation with the nitroso group and the negative end of the oxygen molecule could also be strongly chemisorbed to the MS surface which must be the possible explanation for the disappearance of -N=O peak and the mode of adsorption was explained in Figure 20.

$$R - N - N = O \leftrightarrow R - N^{+} = N - O^{-} \quad (7)$$

As chloride ions are more strongly adsorbed on the iron surface than sulphate ions, the cationic form of the *N*-nitroso inhibitor molecule can adsorb on the metal surface without much difficulty in HCl as compared to H_2SO_4 [24, 25] thereby accounting for high inhibitor efficiency in HCl medium than in H_2SO_4.

According to Frumkin [30], Iofa[31] and Damaskin et al[22]. These inhibitors exist in either as neutral molecules or in the form of protonated cations. The neutral molecules adsorb on the metal surface due to the sharing of lone pair of electrons on nitrogen atoms and the metal surface. The cationic inhibitor molecules electrostatically interact with the negatively charged metal surface through the positive charge on the nitrogen atom. Due to smaller degree of hydration, chloride ions are specifically strongly adsorbed and thereby create excess negative charge towards cationic inhibitor molecules in solution which are strongly adsorbed. However, the SO_4^{2-} ions with high degree of hydration are weakly adsorbed in general and have little space for organic molecules to adsorb. Hence, higher synergistic inhibition is expected for anion of Cl^- type. For the reason stated above the adsorption is greater from 1N HCl solutions than from 1N H_2SO_4, which leads to higher inhibition efficiency values in HCl medium.

In the present study, various adsorption isotherms were tested and it was found that the adsorption of the inhibitors on the surface of mild steel follows the Langmuir adsorption isotherm and Tempkin isotherm. A plot of $\log\theta/1-\theta$ vs logC is found to be linear for Langmuir isotherm, similarly, for Tempkin isotherm; a plot of θ vs logC would be linear. Both Langmuir isotherm and Tempkin isotherm are shown in Figures 21 to 24, respectively.

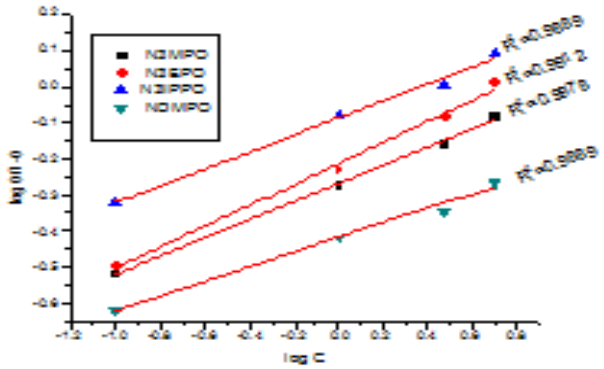

Figure 21: The Langmuir Isotherms for the Adsorption of Inhibitors in 1N H_2SO_4 Solution

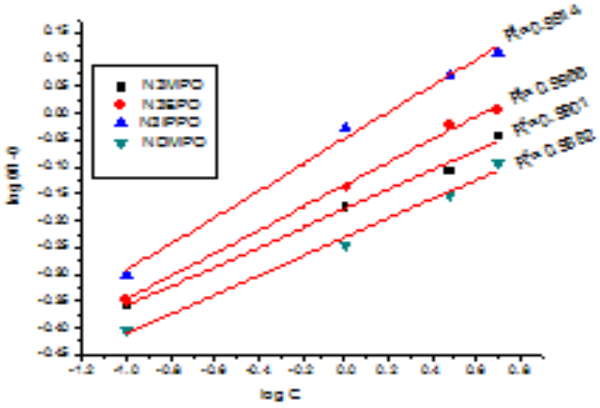

Figure 22: The Langmuir Isotherms for the Adsorption of Inhibitors in 1N HCl Solution

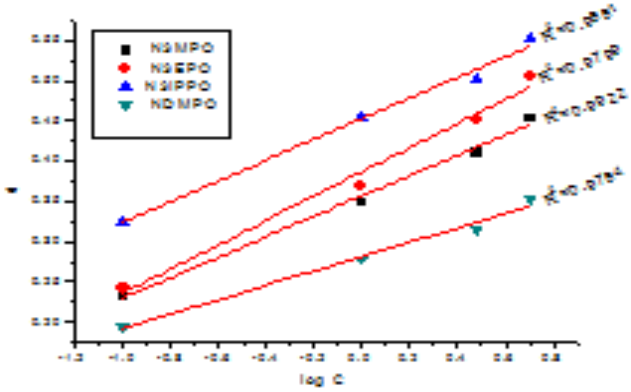

Figure 23: The Tempkin Isotherms for the Adsorption of Inhibitors in 1N H_2SO_4 Solution

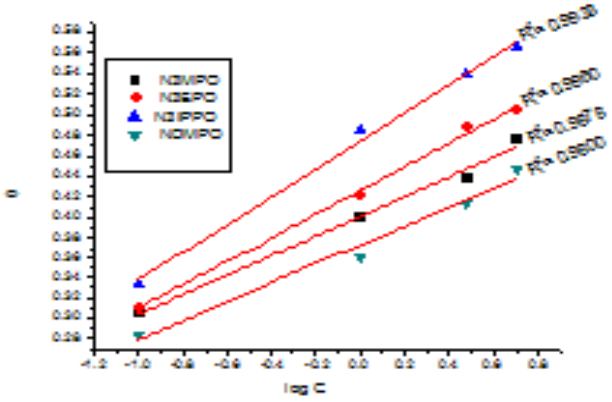

Figure 24: The Tempkin Isotherms for the Adsorption of Inhibitors in 1N HCl Solution

Surface Analysis

Figure 25b shows the scanning electron micrographic image (SEM) of the steel in1N H_2SO_4. A close inspection of the figure reveals two important features: Scattered depression (shown by the arrow) indicating pitting type corrosion and heaps of corrosion products resembling the formation of granular corrosion. The SEM image of the steel in N3IPPO and N3EPO are shown in Figures 25a and 25c.

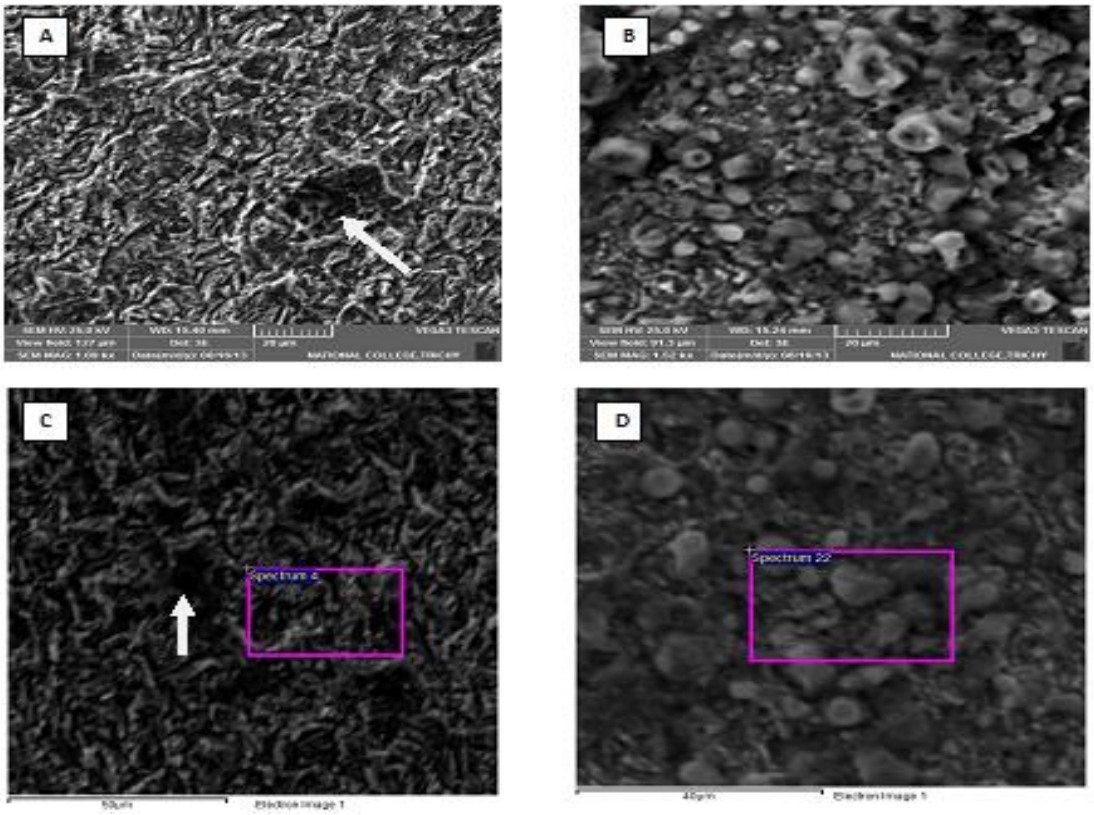

Figures 25: Show the SEM/EDS Image of Uninhibited MS Surface (A and B)
MS Surface Inhibited by N3IPPO (C) and N3EPO (D)

As can be seen in the figure, a finely distributed granular lower layer and a second more loosely distributed bigger-grained solid upon it. The lower layer is probably the inhibitor molecule adsorbed uniformly on the surface which is responsible for protection against corrosion. The lump like upper granules might be precipitation of iron sulphates that were formed on the uncovered sites of the first layer.

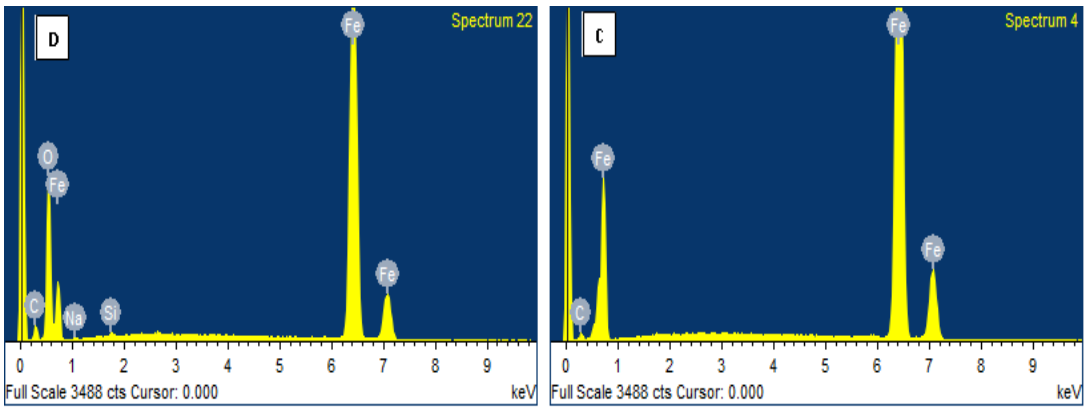

Element	Weight%	Atomic%
C K	8.80	19.32
O K	31.57	52.04
Na K	0.51	0.59
Si K	0.30	0.28
Fe K	58.81	27.77
Totals	**100.00**	

Element	Weight %	Atomic %
C K	6.51	24.46
Fe K	93.49	75.54
Totals	**100.00**	

Figures 26: Show the EDS Image of Uninhibited MS Surface (B) MS Surface Inhibited by N3EPO (D)

When compared with uninhibited EDS, the weight percentage of C and O has increased in the inhibited EDS data where as the percentage of Fe has decreased. This clearly proves the adsorption of organic molecule notably anchored with oxygen on the MS surface.

CONCLUSIONS

A new class of piperidin-4-one based compounds *viz*., N3MPO, N3EPO, N3IPPO and NDMPO act as an inhibitors in both the acids (1N HCl and 1N H_2SO_4) but more effectively in HCl. The inhibition efficiency increases with the increase in concentration of the inhibitor. The inhibition efficiency is temperature dependent and it increases up to 323K, which corroborates that the chemisorption is responsible for inhibitive action. With the rise in immersion time, the IE% increases up to 12 h and remains constant thereafter. Polarisation data showed that these inhibitors affect both cathodic and anodic process and hence they act as mixed type inhibitors. EIS studies revealed that when the concentration of the inhibitor is raised, the IE(%) and R_{ct} values tend to raise but C_{dl} value decreases. Adsorption of inhibitors on the steel surface from 1N H_2SO_4 and 1N HCl follows the Langmuir isotherm and Tempkin isotherm, indicating that the main inhibition process occurs *via* adsorption. The negative value of ΔG°_{ads} obtained from thermal studies indicates that these inhibitors spontaneously adsorbed on the mild steel surface.

REFERENCES

1. S. Muralidharan, R. Chandrasekar and S.V.K.Iyer, *Proc. Indian. Acad. (Chem. Sci).*,**112** (2000) 127.
2. S. Sankarapapavinasam, F. Pushpanathan and M. F. Ahmed, *Corros. Sci.*, **32** (1989) 193.
3. K. F. Khaled, K.Babic-Samardzija and N.Hackerman, *J. Electrochem.*, **34** (2004) 697.
4. K. Rathidevi, A.Selvaraj and T.Mohamed Ikramuddeen. *Int. J. Sci.Research*, (2011) 160 – 163.
5. A. Ilamparithi, S. Ponnuswamy and A. Selvaraj, *International Journal of Applied and Natural Sciences* **3** (2014) 63.
6. T. Ravindran, R. Jeyaraman, R.W. Murray and M. Singh, *J. Org. Chem.* **56** (1991) 4833.
7. R. Jeyaraman, J. C. Thenmozhiyal, R. Murugadoss and M. Muthukumar. *J. Indian Chem. Soc*. **76** (1999) 527.
8. M. Gdaniec, M.J. Milewska and T. Polonski *J. Org. Chem.* **60** (1995) 7411.
9. R. Vijayalakshmi, M. Muthukumar, S. Ponnuswamy, and R. Jeyaraman, *Indian J. Chem.* **45B** (2006) 2720.
10. S.S. Ilango, Ph.D. Thesis, Bharathiar University, India (2012).
11. P. Sakthivel, Ph.D. Thesis, Bharathiar University, India (2014).

12. C. R. Noller and V. Baliah. *J. Am. Chem. Soc.*, **70** (1948) 3853.
13. V. Baliah, R. Jeyaraman and L. Chandrasekaran *Chem. Rev*. **83** (1983) 379.
14. S.S. Ilango, S. Ponnuswamy and T. Viswanathan. *Indian J. Heterocyclic Chem*. **20** (2010) 17.
15. T. Kavitha, M. Thenmozhi, S. Ponnuswamy, P. Sakthivel and M. N. Ponnuswamy *Acta Cryst.* **E65** (2009) 1765.
16. T. Kavitha, S. Ponnuswamy, P. Sakthivel, K. Karthik and M. N. Ponnuswamy. *Acta Cryst.* **E65** (2009) 1420.
17. S. Ponnuswamy, M. Venkatraj, R. Jeyaraman, M. Sureshkumar, D. Kumaran and M.N. Ponnuswamy *Indian J. Chem.* **41B** (2002) 614.
18. S.A. Umoren, I.B. Obot, E.E. Ebenso and N.O. obi-Egbedi, *Desalination*. **250** (2009) 225.
19. G.K. Gomma, Master. *Chem. Phys.* **55**(1998) 241.
20. Y. Harek and L. Larabi, *Kem. Ind.* **53** (2004) 55.
21. E.E. Oguzie, Master. *Chem. Phys.* **87** (2004) 212.
22. Boris B. Damaskin, Oleg A. Petrii and Valerii. V. Batrakov, *"Adsorption of Organic Compounds on Electrodes", Plenum Press, New York, London,* (1971) 262 – 266.
23. K.Aramaki, M.Haghwara and H.Nishihara, Corros. Sci., **27** (1987) 487.
24. H.Ma, S. Chen, B. Yin, S. Zhao and X. Liu, *Corros. Sci.* **45** (2003) 867.
25. R. Solmaz, M.E. Mert, G. Kardas, B. Yazichi and M. Erbil, *Acta Phys. Chem. Sinica* **24** (2008) 1185.
26. V. Ramesh Salian and A.V. Adhikari, *Corros. Sci.* **50** (2008) 55.
27. T. Tsuru, S. Haruyama and Boshoku Gijutsu. *J. Japan Soc. Corros. Eng.* **27** (1978) 573.
28. J.Mallika, Ph.D. Thesis, Bharathiyar University, India (2002).
29. J.Ravichandran, Ph.D. Thesis, Bharathiyar University, India (2006)
30. A.N. Frumkin, *Vestn. Mosk. Gos. Univ.*, **9** (1952) 37.
31. Z.A. Iofa, *Vestn. Mosk. Gos. Univ.*, **2** (1956) 139.

APPENDICES

Table 1: Inhibiting Efficiency from Weight Loss Measurements

Inhibitor+40 ml Ethyl Alcohol	Concentration (mM)	H_2SO_4			HCl		
		Weight Loss (mg)	Corrosion Rate (mm /y)	IE%	Weight Loss (mg)	Corrosion Rate (mm /y)	IE%
N3MPO	Blank 1N H_2SO_4+40 ml Ethyl alcohol	7.715	11.436		10.95	16.232	
	0.1	5.92	8.776	23.32	7.612	11.284	30.48
	1.0	5.012	7.43	35.03	6.556	9.718	40.13
	3.0	4.54	6.730	41.15	6.148	9.113	43.85
	5.0	4.22	6.257	45.36	5.736	8.503	47.62
N3EPO	0.1	5.84	8.657	24.30	7.547	11.187	31.08
	1.0	4.851	7.191	37.12	6.328	9.38	42.21
	3.0	4.23	6.27	45.17	5.612	8.319	48.74
	5.0	3.812	5.651	50.58	5.430	8.049	50.41
N3IPPO	0.1	5.212	7.726	32.44	7.298	10.819	33.35
	1.0	4.204	6.232	45.51	5.646	8.370	48.44
	3.0	3.842	5.695	50.20	5.037	7.467	54.00
	5.0	3.462	5.132	55.12	4.765	7.064	56.48
NDMPO	0.1	6.214	9.211	19.45	7.85	11.637	28.31
	1.0	5.569	8.255	27.82	6.98	10.347	36.26
	3.0	5.29	7.842	31.43	6.42	9.517	41.37
	5.0	4.99	7.397	35.32	6.06	8.983	44.66

Table 2: Effect of Immersion Period on the 1mM Inhibitors of the Corrosion of MS in H_2SO_4 Media

Immersion Period in h	Blank CR (mm/y)	N3MPO		N3EPO		N3IPP0		NDMPO	
		CR (mm/y)	IE(%)	CR (mm/y)	IE(%)	CR (mm/y)	IE(%)	CR (mm/y)	IE(%)
1	9.051	6.932	23.412	6.333	30.030	5.672	37.333	7.663	15.335
3	17.184	10.727	37.576	10.026	41.655	9.265	46.084	14.102	17.935
6	32.38	16.419	49.293	15.566	51.927	14.654	54.744	19.259	40.522
9	47.582	22.112	53.529	21.107	55.641	20.044	57.875	24.416	48.686
12	62.782	27.804	55.713	26.647	57.556	25.434	59.488	29.574	52.894
24	123.579	54.575	55.838	51.807	58.078	49.993	59.546	57.203	53.711

Table 3: Effect of Addition of 1mM Anions on the Corrosion Inhibition of MS in 1N H_2SO_4

Anions	I_1	(1mM N3MPO)			(1mM N3EPO)			(1mM N3IPPO)			(1mM NDMPO)		
		I_2	I'_{1+2}	S	I_2	I'_{1+2}	S	I_2	I'_{1+2}	S	I_2	I'_{1+2}	S
KCl	9.32	35.03	43.1	1.053	37.12	44.4	1.023	45.51	53.8	1.038	27.82	35.65	1.043
KBr	25.58		54.6	1.112		59.2	1.062		58.31	1.22		50.8	1.052
KI	88.37		93.1	1.32		90.39	1.405		93.78	1.432		95.3	1.221
KCNS	6.98		40.3	1.017		43.2	1.045		51.12	1.027		32.1	1.052
KNO_3	-20.93		14.5	0.9724		17.23	0.9975		25.31	0.969		7.02	0.9784

I_1 = Inhibition efficiency of the anions

I_2 = Inhibition efficiency of the cations (inhibitors)

I'_{1+2} = measured inhibition efficiency of anions plus cations.

S = Synergistic factor

Table 4: Effect of the Temperature and Corrosion Inhibition of MS in H_2So_4 Medium

System	303K		308K		313K		318K		323K	
	CR (mm/y)	IE (%)	CR (mm/y)	IE (%)	CR (mm/y)	IE (%)	CR (mm/y)	IE (%)	CR (mm/y)	IE (%)
Blank	13.319	-	23.00	-	32.367	-	41.423	-	50.245	-
N3MPO	9.542	28.35	13.874	39.68	18.058	44.21	22.092	46.67	26.009	48.23
N3EPO	9.224	30.75	13.032	43.34	16.526	48.94	20.303	50.99	23.873	52.48
N3IPPO	8.438	36.65	12.005	47.80	15.559	51.93	18.817	54.57	22.032	56.151
NDMPO	10.463	21.44	14.897	35.23	19.376	40.13	23.672	42.85	27.747	44.78

Table 5: Thermodynamic Parameter

Inhibitor	E_a ($KJmol^{-1}$)	$\Delta H^{\#}$ ($KJmol^{-1}$)	$\Delta S^{\#}$ ($JK^{-1}mol^{-1}$)
BLANK	52.995	50.394	-56.251
N3MPO	40.321	37.730	-101.236
N3EPO	38.268	35.667	-108.422
N3IPPO	38.670	36.069	-107.783
NDMPO	39.396	36.795	-103.614

Table 6: ΔG^{O} ($KJmol^{-}$)

Inhibitor	303K	308K	313K	318K	323K
N3MPO	-7.784	-9.214	-9.848	-10.268	-10.597
N3EPO	-8.074	-9.600	-10.343	-10.725	-11.054
N3IPPO	-8.741	-10.061	-10.655	-11.105	-11.452
NDMPO	-6.848	-8.727	-9.412	-9.859	-10.225

Table 7: Electrochemical Parameters for MS Corrosion in 1N HCl + 40 ml Ethyl Alcohol with Different Concentrations of the Inhibitor

	Conc. of Inhibitor (mM)	R_{ct} Ohm cm^2	C_{dl} (F) $*10^{-5}$	IE (%)	β_a (mV)	β_c (mV)	I_{corr} ($\mu A/CM^2$)	$-E_{corr}$ (mV)	Corrosion Rate (mm/y)	R_p Ohm	IE (%)
	BLANK	34.3	7.34		81	133	313.7	496.8	1.026	89.43	
N3MPO	0.1	57.09	7.13	39.92	65	135	190.2	495.8	0.6034	137	39.24
	1	61.1	6.75	43.86	80	134	179.0	493.2	0.5836	151.2	42.94
	3	66.4	6.79	48.34	72	127	132.1	493.0	0.4324	230.2	57.89
	5	97.6	5.12	64.85	81	150	110.7	482.9	0.3623	260.3	64.71
N3EPO	0.1	61.2	7.23	43.95	68	134	184.4	496.3	0.7024	123	41.22
	1	69.75	5.69	50.65	71	129	178.4	490.2	0.5121	162	43.13
	3	79.6	5.34	56.91	65	132	128.4	486.4	0.4432	235	59.07
	5	99.8	4.38	65.63	81	144	104.6	480.3	0.3792	255	66.66
N3IPPO	0.1	70.1	7.00	51.07	81	133	210.4	496.8	2.176	98.34	32.93
	1	78.4	6.54	56.25	68	123	182.2	485.5	1.532	179.1	41.92
	3	88.3	5.02	61.16	71	134	110.2	481.0	1.42	240.2	64.87
	5	102.2	4.38	66.43	66	136	98.7	464.1	1.13	250.5	68.53
NDMPO	0.1	54.6	6.34	37.18	71	129	224.3	495.3	1.63	120.1	28.50
	1	60.4	5.73	43.21	68	132	190.4	490.4	1.43	150.3	39.31
	3	71.2	4.78	47.84	75	134	150.3	485.6	1.26	229.8	52.09
	5	90.3	3.9	62.02	79	147	120.2	479.2	1.17	249.6	61.68

Table 8: Electrochemical Parameters for MS Corrosion in 1 N H_2SO_4 + 40 ml Ethyl Alcohol with Different Concentrations of the Inhibitor

	Conc. of Inhibitor (mM)	R_{ct} Ohm cm^2	C_{dl} (F) $*10^{-5}$	IE (%)	β_a (mV)	β_c (mV)	I_{corr} ($\mu A/CM^2$)	$-E_{corr}$ (mV)	Corrosion Rate (mm/y)	R_p Ohm	IE (%)
	BLANK	29.39	3.09		78	145	373.8	511.1	5.596	102.3	
N3MPO	0.1	59.6	3.58	50.68	76	152	247.6	501.3	5.032	90.4	33.76
	1	63.2	3.53	53.50	72	147	212.9	497.2	4.39	120.2	43.04
	3	69.8	3.38	57.89	69	151	177.9	490.3	3.63	143.2	52.40
	5	78.6	3.14	62.61	71	160	142.6	485.4	2.92	170.2	61.85
N3EPO	0.1	61.0	3.47	51.82	76	153	240.0	497.9	6.652	86.45	35.79
	1	67.2	3.21	56.26	67	154	190.3	492.5	4.352	121.4	49.10
	3	73.1	3.28	59.79	70	151	171.8	489.6	3.635	149.7	54.04
	5	82.5	3.06	64.37	61	164	137.8	481.4	3.02	167.9	63.14
N3IPPO	0.1	61.9	2.97	52.52	67	142	215.0	500.3	4.393	117.6	42.48
	1	75.1	2.85	60.87	69	151	182.0	495.1	3.727	139.2	51.31
	3	81.2	2.87	63.81	66	147	145.0	493.4	3.697	145.5	61.21
	5	87.2	2.73	66.29	65	151	125.0	489.7	2.544	202.5	66.56
NDMPO	0.1	48.2	3.28	39.02	68	124	225.2	505.7	4.324	102.1	39.75
	1	59.4	3.24	50.52	81	150	200.3	497.7	3.409	129.0	46.42
	3	68.2	3.16	56.91	69	147	179.8.3	482.9	3.009	147.3	51.89
	5	71.2	2.78	58.72	70	163	150.2	467.4	2.86	180.2	59.82